As originally published in the SMTA Proceedings.

Investigation of Compatibility and Reliability in Low Temperature Soldering for Ball Grid Array Components

Watson Tseng, Chunyu Chang, Coti Chung, Keith Lee, Ken Lin
Shenmao America, Inc.
CA, USA
watson_tseng@shenmao.us

ABSTRACT
Low-temperature soldering (LTS) has gained prominence in the Surface Mount Technology (SMT) industry due to its energy efficiency and enhanced production yields. However, like the transition from leaded to lead-free solder, the increasing adoption of LTS presents compatibility challenges, particularly with Ball Grid Array (BGA) components. This study explores the reliability of different ball-paste combinations for LTS soldering.

Four combinations were investigated: 1) LTS ball with LTS paste, 2) SAC ball with LTS paste, 3) LTS ball with SAC paste, and 4) SAC ball with SAC paste. Testing was conducted using a wafer level package, which causes a large coefficient of thermal expansion (CTE) mismatch with epoxy glass fiber-based printed circuit board (PCB), as test vehicle. Soldering profiles were specified for LTS and SAC pastes. Microsectioning and thermal cycling from -40°C to 100°C were performed, with failure defined as a 20% resistance change. Findings from this investigation suggest that LTS soldering may enhance the reliability of joints in some combinations.

Key words: Low-temperature soldering, compatibility, solder joint reliability, board level reliability.

INTRODUCTION

LTS has gained popularity in the SMT industry in recent years, primarily because of its reduced energy consumption and improved production yields during the soldering process.

Similar to the transition from leaded solder to lead-free solder [1], the increasing adoption of LTS will pose compatibility issues in the industry, particularly with BGA components that attach LTS balls.

In practical scenarios, LTS paste can be used to solder either with LTS ball or SAC ball attached components, or LTS ball attached component can be soldered with SAC paste. However, the reliability of different paste-ball combinations remains largely unexplored.

This study investigated four types of ball-paste combinations; each combination indeed carries its own significant implications within the context of soldering technology:

SAC-SAC, reflowing SAC ball attached component with SAC paste: This configuration represents the most mature technique within the lead-free soldering generation. It reflects well-established and widely adopted practices in the lead-free era, showcasing the reliability and widespread acceptance of SAC soldering technology.

SAC-LTS (hybrid soldering), reflowing SAC ball attached component with LTS paste: This configuration signifies a transitional phase from the well-known SAC soldering to the emerging LTS technology. It reflects a dynamic period of technological evolution where LTS is introduced into existing SAC processes. In recent years, numerous studies and experiments are conducted based on this configuration as it bridges the gap between old and new soldering practices.

LTS-LTS, reflowing LTS ball attached component with LTS paste: This configuration represents the established and mature technique of LTS. In this setup, LTS is employed both as the input/output (I/O) interface on the package and as the connecting medium on the printed circuit board assembly (PCBA). It showcases the reliability and efficacy of LTS as a standalone solution.

LTS-SAC (reverse hybrid soldering), reflowing LTS ball attached component with SAC paste: This configuration exemplifies the backward compatibility of LTS technology. It demonstrates LTS's adaptability to existing SAC processes, allowing for the integration of advanced soldering techniques into established manufacturing environments.

These configurations serve as valuable tools for evaluating and understanding the progression and compatibility of soldering techniques, offering insights into the industry's past, present, and future soldering practices.

EXPERIMENTAL PROCEDURES

Alloy and Properties

In this investigation, three distinct alloys were employed, as detailed in Table 1. The first alloy, denoted as SAC, comprises Sn-3.0Ag-0.5Cu, and was processed into T4 powder form and BGA spheres with a diameter of 0.25mm. The LTS application utilized two separate alloys: LTS-Ball, consisting of Sn-40Bi-1Ag, was fashioned into BGA spheres with a 0.25mm diameter, while LTS-Paste, composed of Sn-57Bi-1Ag, underwent processing into T4 powder for subsequent incorporation into solder paste blends.

The mechanical properties of the three alloys were assessed through a tension test. For each alloy, three test specimens were prepared in the form of rectangular tension test

specimens, as outlined in Figure 1. These specimens featured a gauge length of 32mm and a thickness of 4mm.

The tension test was executed with a displacement rate set at 6mm/min. The resulting data, including the elastic modulus, yield strength, ultimate strength (UTS), and elongation, have been compiled in Table 2, representing the averages derived from the measurements obtained from three specimens for each alloy.

Table 1. Alloy Compositions

Alloy	Sn	Bi	Ag	Cu
SAC	REM.	-	3.0	0.5
LTS-Ball	REM.	40.0	1.0	-
LTS-Paste	REM.	57.0	1.0	-

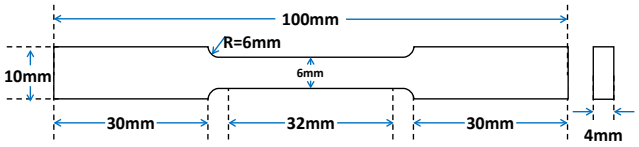

Figure 1 Dimension of tension test specimen

Table 2. Mechanical Properties of Alloys

	SAC	LTS-Ball	LTS-Paste
Yield Strength [MPa]	42.3	69.7	65.3
Ultimate Strength [MPa]	47.3	72.2	67.7
Elongation [%]	43.3	35.8	36.7

Test Vehicle

The Figure 2 shown the test vehicle, BGA package and PCB, used in this study. Table 3 described the characteristics of the BGA package employed for evaluating. The SAC-Ball and LTS-Ball alloys were soldered onto the BGA package, thereby establishing the I/O connections.

The PCB employed for conducting thermal cycling assessments is designed as a two-layer board measuring 77 mm x 77 mm in size, which specifies its layout and dimensions to accommodate up to four components. A total of three PCBs were prepared, resulting in a combined total of 12 BGA packages per test group. The PCB surface finish is configured with organic solderability preservative (OSP) treatment. Each land pattern features a dedicated daisy chain net, and these daisy chain nets originating from each component's patterns are routed to a card edge connector. Soldered connections are employed to facilitate the monitoring of resistance variations within the daisy chain nets throughout the course of thermal cycling testing.

The CTE for both the BGA package and the PCB was determined through Thermal Mechanical Analysis (TMA). The results revealed a CTE of 2.4 ppm/K for the BGA package and 14.5 ppm/K for the PCB. This significant difference in CTE values clearly indicates a notable CTE mismatch between the BGA package and the PCB, highlighting the potential for thermal stress and mechanical strain during temperature fluctuations.

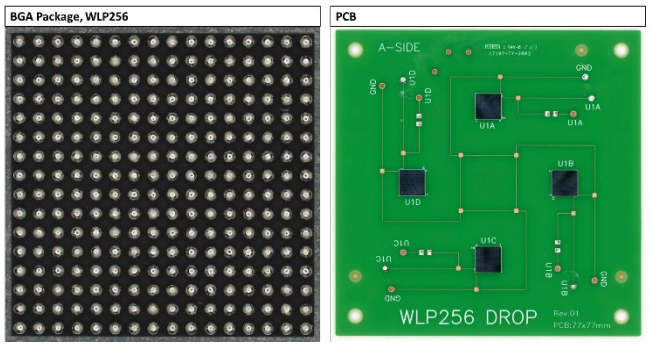

Figure 2 Test vehicle

Table 3. The BGA package test vehicle attributes

Description	Attributes
Package Size	6.4 x 6.4 mm
Substrate Composition	Silicon
Substrate Thickness	0.40 mm
Surface Finish	Copper
Solder Ball Count	256
Solder Ball Pitch	0.40 mm
Solder Ball Diameter	0.25 mm

Stencil Design

The LTS and SAC solder pastes were printed onto the PCB pads through an 80 µm thick stainless-steel stencil. The stencil's apertures were designed with a size of 0.25mm, aiming to attain a paste-to-ball ratio near 50%.

Reflow Profile

The Ramp-Soak-Spike (RSS) profile is a widely used thermal profile in SMT processes, particularly for SAC paste. In our study, we selected a soak time, which is the duration between 150°C and 200°C, of 80 seconds, and a time above 220°C duration of 70 seconds. The peak reflow temperature was set at 240°C, as depicted in Figure 3.

The recommended thermal profile for the LTS paste follows a trapezoidal shape, characterized by a time above 140°C duration of 150 seconds and a peak temperature set at 170°C, as illustrated in Figure 4. The reflow process for all samples in this study was conducted in an ambient air atmosphere.

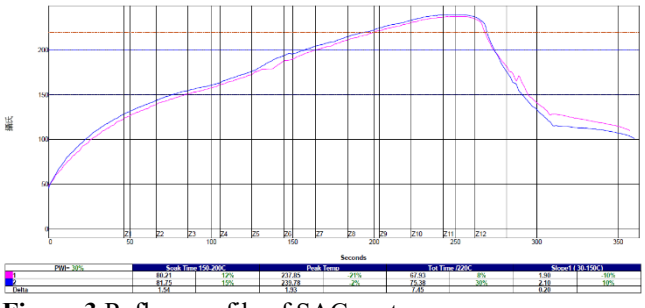

Figure 3 Reflow profile of SAC paste

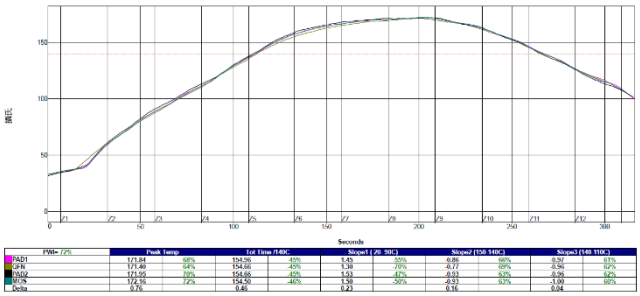

Figure 4 Reflow profile of LTS paste

Test Group

The details of the four paste-ball combinations are summarized in Table 4.

Table 4. Information of test group

Test Group	SAC-SAC	SAC-LTS	LTS-LTS	LTS-SAC
Ball alloy	SAC	SAC	LTS-Ball	LTS-Ball
Bi% in ball	0%	0%	40.0%	40.0%
Paste alloy	SAC	LTS-Paste	LTS-Paste	SAC
Bi% in paste	0%	57.0%	57.0%	0%
Reflow Peak Temp.	240°C	170°C	170°C	240°C
Calculated Joint Bi% after assembly	0%	N/A	43.5%	33.0%
Joint Structure	Homo.*	Hybrid	Homo.*	Homo.*

*Homo. stand for homogeneous

Thermal Cycling Condition

Thermal cycling was performed over a temperature range of -40°C to 100°C, utilizing a ramp rate of 15°C per minute. 100°C is selected instead of 125°C because the temperatures are too close to the solidus point of LTS alloy (137°C). At each extreme temperature, a dwell time of 10 minutes is maintained. The resistance was in-situ monitored with failure definition and a maximum of 20% nominal resistance increase within five consecutive reading scans.

RESULTS AND DISCUSSION

Joints Structure and Composition after Assembly

Table 4 documents the calculated bismuth content within the solder joints and joint structure of each test group post-assembly. These calculations were made considering a paste-to-ball ratio of 48% and a volume fraction of solder alloy in solder paste equal to 50%.

In the case of the SAC-SAC test configuration, assembly is performed at a peak temperature of 240°C. In this scenario, both the solder ball and solder paste liquefy, culminating in the formation of a homogeneous SAC joint that does not contain bismuth.

For the SAC-LTS test configuration, assembly also occurs at a peak temperature of 170°C. During this process, the solder paste is melted and is wetted to SAC ball, leading to the creation of a hybrid joint.

Next, in the LTS-LTS test configuration, the assembly process involves reaching a peak temperature of 170°C. At this temperature, the solder ball and solder paste undergo melting, resulting in the formation of a unified joint with a bismuth content of approximately 43.5%.

Lastly, in the LTS-SAC test configuration, the assembly process necessitates reaching a higher peak temperature of 240°C. At this elevated temperature, both the solder ball and solder paste liquefy, yielding a homogeneous joint with a bismuth content of around 33.0%.

X-ray Observation after Assembly

X-ray examinations of all samples were conducted. These examinations revealed that all joints were aligned and positioned as intended, as shown in Figure 5.

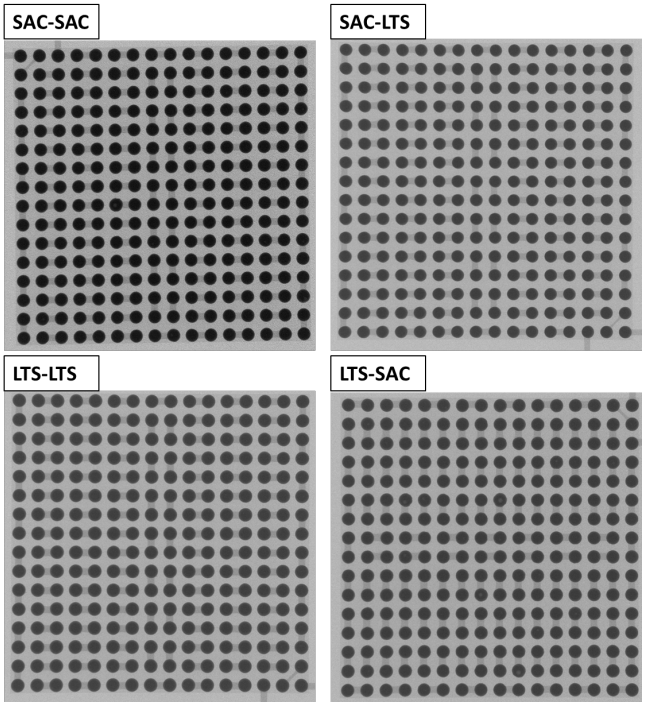

Figure 5 X-ray observation after assembly

Microsectioning after Assembly

A single specimen from each of the test groups underwent microsectioning to investigate the microstructure of the joints, as illustrated in Figure 6. All test groups exhibited favorable joint appearances following assembly. The bismuth content within the solder joints was quantified using Energy Dispersive Spectroscopy (EDS) analysis. To validate the accuracy of the calculated bismuth content, the EDS results are presented in Table 5. Notably, the comparison between the calculated values and the EDS results revealed minimal disparity, affirming the precision of the calculated bismuth content.

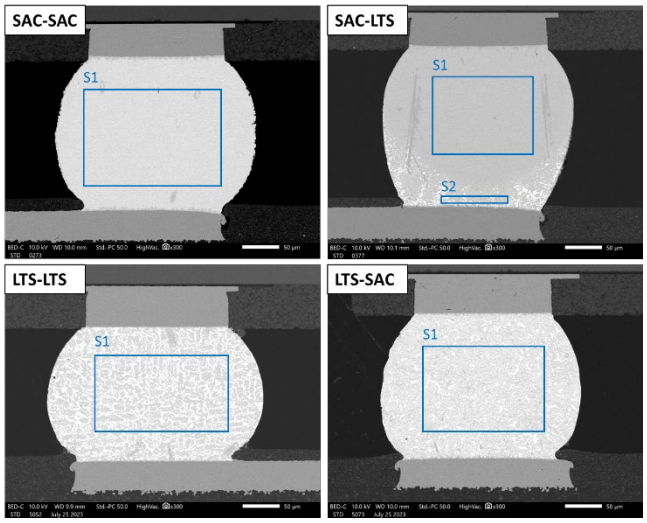

Figure 6 SEM observation after assembly

Table 5. EDS analysis after assembly

Test Group	SAC-SAC	SAC-LTS		LTS-LTS	LTS-SAC
Location	**S1**	**S1**	**S2**	**S1**	**S1**
Sn	94.08	94.57	73.61	55.71	68.27
Bi	-	-	24.57	43.41	28.98
Ag	3.62	3.21	-	-	1.66
Cu	2.3	2.22	1.83	0.88	1.08

The standoff height of each test group was measured. Based on the microsectioning observations, commencing from the leftmost side, Joint 1 is denoted as "Left", Joint 8 is identified as "Middle", and Joint 16 is designated as "Right", as illustrated in Figure 7. The measured results, as detailed in Table 6, indicate that the variation in standoff height among all test legs can be characterized as minimal. The maximum range observed is approximately 4.2 micrometers. This observation suggests that there are no significant warpage issues with the samples following the assembly process.

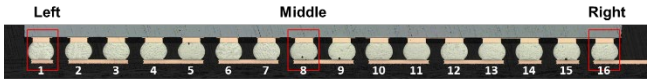

Figure 7 Denotation of standoff measurement

Table 6. Standoff measurement after assembly

Test Leg		SAC-SAC	SAC-LTS	LTS-LTS	LTS-SAC
Standoff Height (um)	**Left**	212.6	180.7	195.6	203.4
	Middle	216.8	180.9	195.4	206.1
	Right	216.3	179.3	193.4	206.1
	Range	4.2	1.6	2.2	2.7

Thermal Cycling Test Results

Table 7 presents data on failure cycles and characteristic life for each of the test legs, while Figure 8 illustrates the Weibull distribution of the results. The findings indicate that the SAC-LTS test group, characterized by a hybrid joint structure, exhibits the shortest characteristic life. In contrast, the remaining three test groups, featuring homogeneous joint structures, display characteristic life sequences from lowest to highest as follows: SAC-SAC, LTS-LTS, and finally, LTS-SAC.

Table 7. Thermal Cycling Test Results

Leg ID	SAC-SAC	SAC-LTS	LTS-LTS	LTS-SAC
Failure Cycle	494	139	492	1072
	557	152	618	1109
	618	154	626	1223
	655	158	728	1259
	692	177	744	1284
	699	202	818	1302
	716	203	841	1316
	766	208	851	1439
	785	229	858	1536
	826	256	880	1544
	917	260	988	1709
	946	332	1393	1846
Characteristic Life	777	224	892	1474

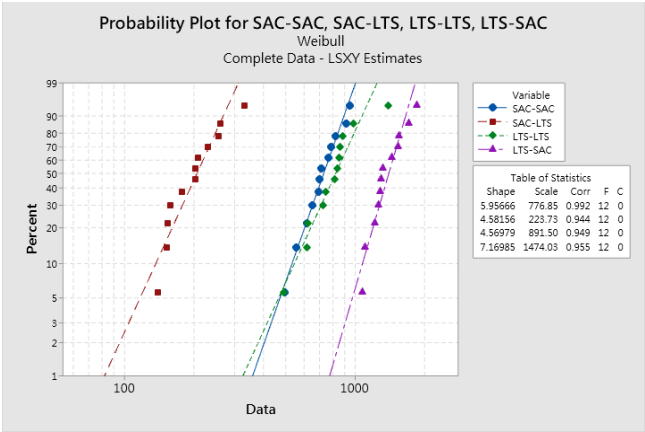

Figure 8 Weibull distribution of thermal cycling test

X-ray Observation after Thermal Cycling Test

X-ray observations were conducted on the last-failed sample of all test groups. In three of the test groups featuring a homogeneous joint structure, the joints have remained stable and in their intended positions as-like post-assembly. However, in the test group with a hybrid joint structure, a phenomenon of solder ball drift, previously observed in a prior study [2], is evident, as depicted in Figure 9. In this figure, we have enlarged and focused on the 6x6 grid of joints located in the bottom-left corner, with an added grid overlay to underscore the solder ball drift phenomenon. It is noteworthy that while the drift occurs in a seemingly random fashion, the overall movement appears to converge toward the center of the package.

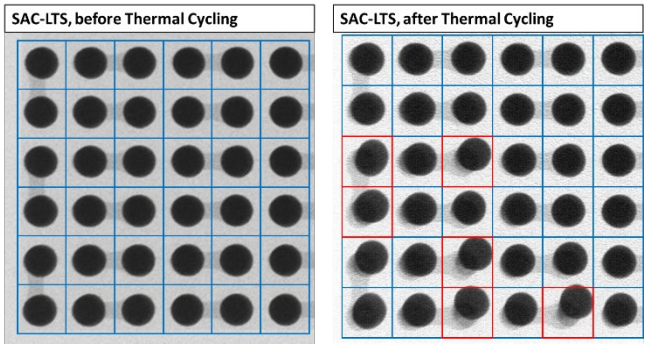

Figure 9 X-ray Image of SAC-LTS after Thermal Cycling

Microsectioning after Thermal Cycling Test

After conducting X-ray observations, all last-failed samples were subjected to microsectioning and subsequent examination via SEM, as illustrated in Figure 10 to Figure 13.

In the case of the SAC-SAC test group, cracks were observed at both the interface between the solder and PCB side Intermetallic Compounds (IMC) and within the solder near the package side. Notably, the roundness of the joints remained intact for these three test legs.

In the hybrid joint structure test group SAC-LTS, it has been observed that the joints undergo distortion during testing. Specifically, the SAC portion of the joint is extruded towards the center of the package. Additionally, cracks have been observed within the LTS portion of the joint, particularly at the interface between the IMC and the LTS material.

Conversely, in the LTS-LTS test group, which features a homogeneous joint structure, a majority of the observed cracks were found to be situated at the interface between the solder and the PCB side IMC.

For the LTS-SAC test group, another homogeneous joint structure containing bismuth, most of the cracks were located within the solder near the package side.

The standoff height of each test leg was measured following the thermal cycling test, as detailed in Table 8. Due to the presence of induced cracks during the thermal cycling test, the standoff height was measured from the package pad to the PCB pad. The results revealed that the variation in standoff height remained minimal after the thermal cycling test. This observation suggests that, despite the CTE mismatch between the BGA package and the PCB, both units are capable of returning to its normal condition after experiencing thermal fluctuations.

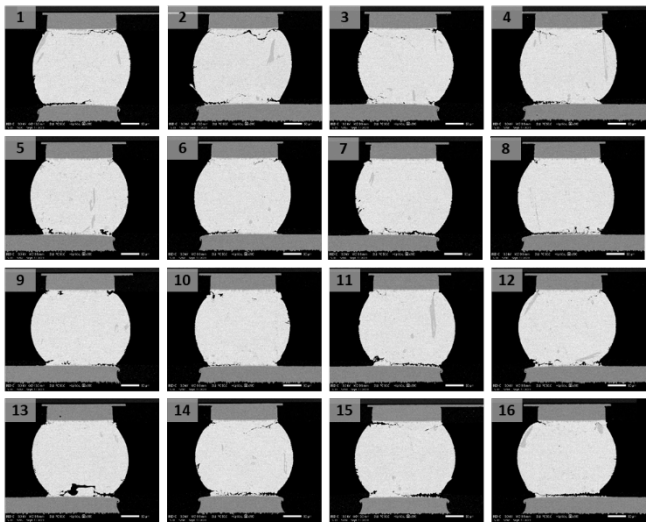

Figure 10 SEM observation of SAC-SAC last-failed sample

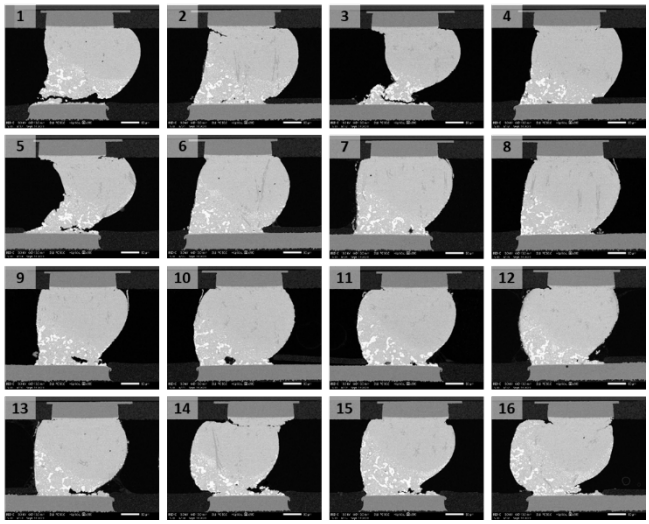

Figure 11 SEM observation of SAC-LTS last-failed sample

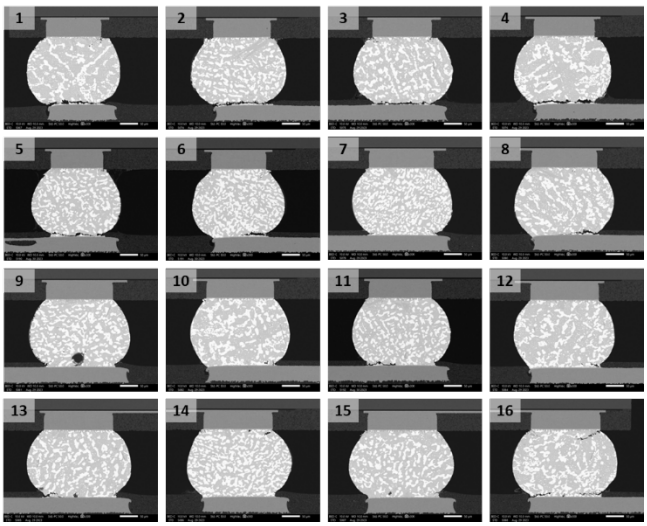

Figure 12 SEM observation of LTS-LTS last-failed sample

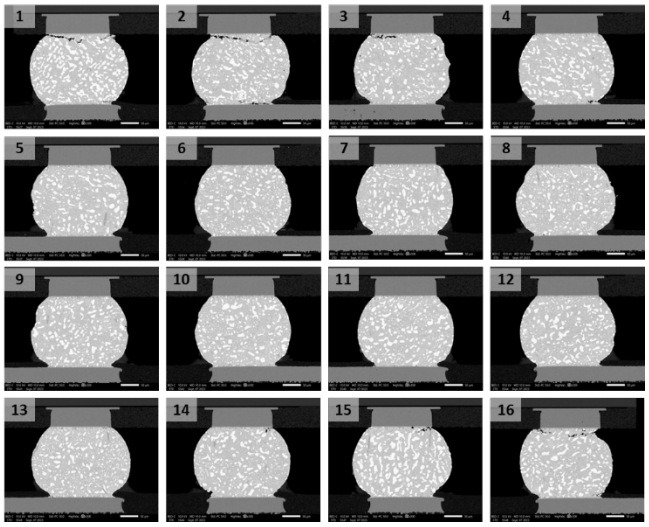

Figure 13 SEM observation of LTS-SAC last-failed sample

Table 8. Standoff measurement after thermal cycling

Test Leg		SAC-SAC	SAC-LTS	LTS-LTS	LTS-SAC
Standoff Height (um)	Left	196.0	189.3	214.7	210.2
	Middle	195.6	188.0	217.3	210.2
	Right	193.3	189.8	216.5	211.1
	Range	2.7	1.8	2.6	0.9

Discussion of Thermal Cycling Test Results

By comparing the standoff height measurements of pre- and post-thermal cycling test for each test group, it becomes evident that the warpage remained negligible. This observation indicates that the thermal stress resulting from the CTE mismatch is effectively transferred to the solder joints, and no distortion has been detected either at the package or the PCB.

In Figure 14, we have illustrated the stress conditions within the joint located farthest from the center during thermal fluctuations. To simplify the representation, the joint is represented as a column. The PCB possesses a higher CTE compared to the package . This implies that as temperature rises, the PCB undergoes more significant expansion than the silicon-based package.

As a result, the joint will experience distortion due to the CTE mismatch. During this distortion process, two of the corners of the joint become subjected to tension stress when the temperature increases, while the other two corners experience tension stress when the temperature shifts from hot to cold. This cyclic stress due to temperature fluctuations contributes to the mechanical behavior of the joint. It's worth noting that the extent of distortion becomes more pronounced as the joint's location moves farther away from the center of the package, exacerbating the distortion behavior in these peripheral areas.

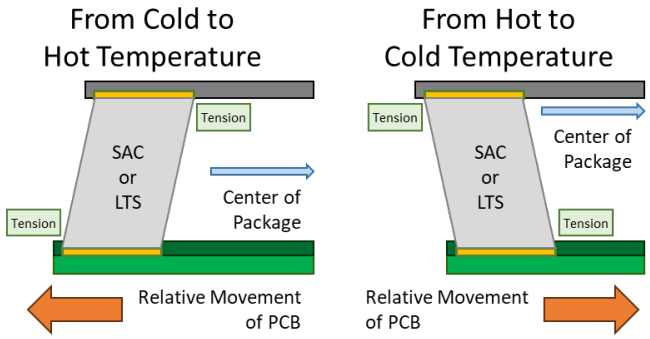

Figure 14 Stress condition within the joint during thermal fluctuation

Figure 10 provides valuable insights into the SAC-SAC test group, where it is evident that the majority of cracks are situated at the corners that experienced tension stress during the transition from low to high temperatures. These cracks typically initiate at the corners and propagate along the PCB side IMC or within the solder matrix, closer to the package. Interestingly, this phenomenon is not as prominently observed in bismuth-contained homogeneous test groups.

From Table 4, we can find that the yield strength and the UTS of SAC are lower than that of LTS. When the thermal stress surpasses the yield stress of the joint materials, it can lead to permanent deformation in the joints. If the thermal stress exceeds the UTS of the joint materials, it may result in the initiation of cracks within the solder joints. Hence, if the same level of thermal stress is applied to both bismuth-contained homogeneous joints and bismuth-free homogeneous joints, it is more likely that permanent deformation will be induced in the bismuth-free homogeneous joints. This is exemplified by the SAC-SAC test group in this study, where the absence of bismuth in the solder alloy makes it more susceptible to permanent deformation under the same thermal stress conditions when compared to bismuth-contained joints.

In the case of homogeneous joints, the tension stress induced during temperature fluctuations should ideally be equally distributed among the corners of the joint. In materials that are prone to deformation, such as SAC in this context, all corners have similar properties for crack initiation. As a result, when cracks initiate in SAC homogeneous joints, they may not propagate throughout the entire joint. Consequently, cracks can be observed in SAC homogeneous joints at both the package side and PCB side. Conversely, in bismuth-contained homogeneous joints, cracks tend to propagate as they initiate. Therefore, only one side, either the package side or the PCB side, will typically exhibit cracks, depending on where the initial crack formation occurs.

Notably, prior studies [3-6] have indicated that as the temperature increases, the elastic modulus and the UTS of SAC305 solder tend to decrease. This suggests that SAC becomes more susceptible to deformation or cracking during periods of elevated temperature. This also helps explain why cracks are less likely to be induced during the transition from

hot to cold temperatures, as the mechanical properties of SAC become stronger during this temperature shift.

In another previous study done by Takao, H. et al. [7] show that, the low ductility observed in bismuth-containing tin-based alloys is primarily attributed to the solid solution hardening effect. This issue can be mitigated by maintaining a bismuth content within the range of 30-45%. This study offers an additional perspective that helps explain why the thermal cycling life of bismuth-containing test groups tends to outperform the SAC-SAC test group.

When we compare the two bismuth-contained homogeneous test groups, LTS-LTS and LTS-SAC, it becomes evident that the test group with lower bismuth content exhibits superior life cycle performance. This observation can also be explained by differences in their mechanical properties. A previous study conducted by Cai et al. [8], which demonstrated that the UTS of SnBi alloy initially increases with increasing Bi content, reaching its maximum value at 17 wt.%. However, as the Bi content exceeds 17 wt.% and approaches 58 wt.%, the UTS starts to decline. This information suggests that the UTS of LTS-SAC may be higher than that of LTS-LTS, resulting in the improved life cycle performance observed in the SAC-LTS test group.

In the case of the SAC-LTS test group, which features a hybrid joint structure, it exhibits the shortest failure cycle among all the test groups. Figure 9 and Figure 13 suggest that this test group experiences random solder joint drift issues. This is attributed to the fact that, in a hybrid joint, there are two different materials within the joint, each with distinct mechanical properties.

Assuming a paste-to-ball ratio of 50% and that the solder paste contains 50% of the solder alloy, we can estimate that the SAC ball's volume comprises approximately 80% of the joint volume, with the LTS alloy from the solder paste accounting for the remaining 20%. However, during the reflow process, several factors come into play. Firstly, there's the melting of LTS, and secondly, bismuth penetration occurs into the SAC portion.

As a result of these processes, the LTS portion within the joint exceeds the initial 20%. Additionally, when LTS paste wets a SAC ball, the flux's influence causes LTS to spread along the surface of the SAC ball, leading to a higher level of bismuth penetration at the sides of the joint compared to the middle portion. The term "Bi mixing," as described in previous research [9], is used to describe this phenomenon of bismuth penetration into the solder joint.

To simplify the visualization of the joint structure, we can conceptualize it as a two-layer column, where bismuth penetration is uniform between the sides and the middle, as illustrated in Figure 15.

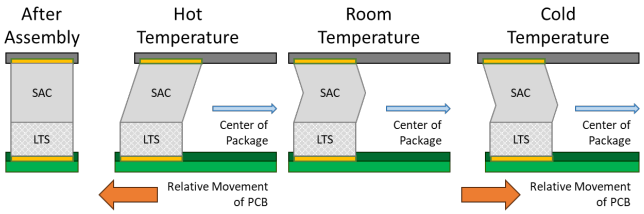

Figure 15 Illustration for hybrid joints

As the process of thermal cycling initiates, thermal stress is introduced into the solder joints, resulting in distortion similar to what is observed in homogeneous joints. In cases where the thermal stress surpasses the yield strength of one of the materials, specifically SAC in this context, permanent deformation occurs. When the thermal cycling transitions from hot to cold temperatures, LTS can return to its original state, but SAC does not fully recover. Some residual deformation remains in the joint shape. As thermal cycling continues, this cumulative deformation contributes to the condition illustrated in Figure 13, where the joints are extruded towards the inner side of the package.

As SAC deforms during thermal cycling, an important consideration is that the LTS paste is soldered to the SAC ball. Consequently, the LTS portion that is connected to the SAC will deform in harmony with the SAC portion, considering the effects of bismuth penetration. This mutual deformation between the SAC and LTS components highlights the interconnected behavior of the materials within the joint structure, further contributing to the joint's response to thermal stress. Eventually, if the deformation of SAC cannot withstand the induced thermal stress, cracks will form in the necking region of the SAC layer. Conversely, if the thermal stress exceeds the strength of the LTS layer, cracks will initiate in the LTS layer. Based on our observations in Figure 13, it appears that the majority of the joint cracks are located within the LTS portion.

The phenomenon of random solder ball drift can be attributed to the irregularities in Bi mixing within the solder joint. Despite verifying Bi mixing through microsectioning post-assembly, consistent Bi mixing at the same joint position cannot be ensured under identical reflow conditions. The penetration of bismuth is unpredictable and tends to vary randomly within the joint.

Since Bi mixing significantly influences the deformation of the solder joint, the solder joint drift locations also become random due to this variability in Bi penetration. The erratic distribution of bismuth within the joint disrupts the uniformity of deformation, resulting in the observed random drift of solder balls, further emphasizing the role of Bi mixing in this phenomenon.

The discussion presented above provides a hypothesis to explain why hybrid joints may exhibit a more pronounced response to thermal fatigue. However, due to the complexity of the interactions involved in solder joints, further in-depth studies are required to gain a deeper understanding of the

phenomenon. Conducting more extensive research will be essential for elucidating the intricate mechanisms at play within hybrid joints during thermal cycling and for verifying the hypotheses proposed. This continued investigation will contribute to advancing our knowledge of solder joint behavior and enhancing the reliability of electronic assemblies subjected to thermal stress.

CONCLUSIONS

In this study, we conducted an investigation into the solder joint reliability across various combinations of SAC ball, SAC paste, LTS ball, and LTS paste to assess the compatibility of LTS soldering techniques. In the test vehicle characterized by a significant CTE mismatch, we made several key findings:

1. Homogeneous joint structures outperform hybrid joints: We observed that solder joints with a homogeneous composition demonstrated superior life performance compared to joints with a hybrid composition.

2. Bismuth-containing joints exhibit better reliability: Solder joints containing bismuth showed improved life performance in comparison to bismuth-free joints. This is primarily attributed to the enhanced mechanical properties associated with bismuth-containing alloys.

3. Lower bismuth content enhances reliability: Among joints with bismuth content, those with lower bismuth content exhibited better life performance. This trend aligns with the observation that as the bismuth content increases beyond 17 wt.% and approaches 58 wt.%, the mechanical properties of the solder tend to decline.

4. Deformation in hybrid joints results from SAC tiny deformation accumulation: The deformation observed in hybrid joints is a consequence of the accumulation of tiny deformations within the SAC layer, leading to the extrusion of SAC. If the displacement is significant enough, it can induce cracks in the LTS portion of the joint.

These findings contribute to our understanding of solder joint reliability and the factors that influence it, particularly in the context of LTS soldering techniques.

REFERENCE

[1] J. Nguyen, D. Geiger, D, Rooney, and D. Shangguan, "Backward Compatibility Study of Lead-Free Area Array packages with Tin-Lead Soldering Processes," Proceedings of APEX, S09-03, Anaheim, CA, 2006.

[2] Richard Coyle, Martin Anselm, Faramarz Hadian, Sahana Kempaiah, Anto Raj, Richard Popowich, Lenora Clark, Jason Fullerton, and Charmaine Johnson, “The Effect of Peak Reflow Temperature on Thermal Cycling Performance and Failure Mode of Hybrid Low Temperature Solder Joints,” Proceedings of SMTAI 2021, 386-399, Minneapolis, MN, November 2021.

[3] M. M. Basit, M. Motalab, J. C. Suhling and P. Lall, "The effects of aging on the Anand viscoplastic constitutive model for SAC305 solder," 2014 14th ITherm, Orlando, FL, , pp. 112-126.

[4] Basit, M. M., Motalab, M., Suhling, J. C., Lall, P., “Viscoplastic Constitutive Model for Lead-Free Solder Including Effects of Silver Content, Solidification Profile, and Severe Aging,” Proceedings of InterPACK 2015, pp. 1-18, San Francisco, CA, July 6-9, 2015.

[5] M. S. Alam, M. Basit, J. C. Suhling and P. Lall, "Mechanical characterization of SAC305 lead free solder at high temperatures," 2016 15th IEEE ITherm, Las Vegas, NV, 2016, pp. 755-760.

[6] P. Lall, V. Mehta, J. Suhling and K. Blecker, "High Strain-Rate Properties for SAC305 at Cold Operating Temperatures down to -65°C," 2020 19th IEEE ITherm, Orlando, FL, 2020, pp. 1073-1083.

[7] Takao, H. et al., “Mechanical Properties and Solder Joint Reliability of Low-Melting Sn-Bi-Cu Lead Free Solder Alloy”. R&D Review of Toyota CRDL, Vol. 39, No. 2 (2004), pp. 49-56.

[8] Cai, S., Luo, X., Peng, J. et al., “Deformation mechanism of various Sn-xBi alloys under tensile tests”. Adv Compos Hybrid Mater 4, 379–391 (2021).

[9] Scott Mokler, Ph.D., P.E., Raiyo Aspandiar, Ph.D., Kevin Byrd, Olivia Chen, Satyajit Walwadkar, Kok Kwan Tang, Mukul Renavikar and Sandeep Sane, "The Application of Bi-Based Solders for Low Temperature Reflow to Reduce Cost While Improving SMT Yields in Client Computing Systems," 2016 SMTA International, Rosemont, IL, 2016, pp. 318-326.